



**HAL**  
open science

## Community composition predicts photogrammetry-based structural complexity on coral reefs

J. Carlot, A. Rovère, E. Casella, D. Harris, C. Grellet-Muñoz, Y. Chancerelle,  
E. Dormy, L. Hédouin, V. Parravicini

► **To cite this version:**

J. Carlot, A. Rovère, E. Casella, D. Harris, C. Grellet-Muñoz, et al.. Community composition predicts photogrammetry-based structural complexity on coral reefs. *Coral Reefs*, 2020, 39, pp.967-975. 10.1007/s00338-020-01916-8 . hal-02715266

**HAL Id: hal-02715266**

**<https://univ-perp.hal.science/hal-02715266>**

Submitted on 26 Nov 2020

**HAL** is a multi-disciplinary open access archive for the deposit and dissemination of scientific research documents, whether they are published or not. The documents may come from teaching and research institutions in France or abroad, or from public or private research centers.

L'archive ouverte pluridisciplinaire **HAL**, est destinée au dépôt et à la diffusion de documents scientifiques de niveau recherche, publiés ou non, émanant des établissements d'enseignement et de recherche français ou étrangers, des laboratoires publics ou privés.

1 **Community composition predicts photogrammetry-based structural**  
2 **complexity on coral reefs**

3

4 J. Carlot<sup>1-2\*</sup>, A. Rovère<sup>3-4</sup>, E. Casella<sup>3-4</sup>, D. Harris<sup>5</sup>, C. Grellet-Muñoz<sup>1-3</sup>, Y. Chancerelle<sup>1-2</sup>,  
5 E. Dormy<sup>6</sup>, L. Hedouin<sup>1-2</sup>, V. Parravicini<sup>1-2</sup>

6

7 <sup>1</sup>PSL Université Paris: EPHE-UPVD-CNRS, USR 3278 CRIOBE, BP 1013, 98729 Papetoai,  
8 Moorea, French Polynesia

9 <sup>2</sup>Laboratoire d'Excellence « CORAIL »

10 <sup>3</sup>Centre for Marine Environmental Sciences (MARUM), Bremen University, Bremen,  
11 Germany.

12 <sup>4</sup>Leibniz Centre for Tropical Marine Research, Bremen, Germany.

13 <sup>5</sup>The University of Queensland, School of Earth and Environmental Sciences, Brisbane,  
14 Queensland, Australia.

15 <sup>6</sup>Department of Mathematics and Applications, CNRS UMR 8553, Ecole Normale Supérieure,  
16 Paris, France

17

18 **Keywords**

19 Coral Complexity – Rugosity measures – Photogrammetry – Reef ecology – Modeling

20

21 \*Corresponding author: Jérémy Carlot,  
22 PSL Research University  
23 EPHE-UPVD-CNRS  
24 USR 3278 CRIOBE  
25 BP 1013, 98729 Papetoai, Moorea, French Polynesia  
26 Laboratoire d'Excellence « CORAIL »  
27 E-mail: [Jeremy.carlot@hotmail.fr](mailto:Jeremy.carlot@hotmail.fr)

28 **Abstract**

29           The capacity of coral reefs to provide ecosystem services, to keep their diversity and  
30 their productivity are related to their three-dimensional structural complexity. This parameter  
31 is also correlated to total fish biomass, to the general reef resilience to external stresses and to  
32 their ability to dissipate wave energy. However, information on structural complexity (also  
33 defined as reef rugosity) has been uncommonly assessed in historical monitoring programs,  
34 with the result that the long-term trend of this variable is generally unavailable. In this study,  
35 we show that it is possible to predict and hindcast the three-dimensional complexity of coral  
36 reefs by combining photogrammetry, statistical modeling and historical benthic community  
37 data. We calibrated a lasso generalized linear model to predict structural complexity obtained  
38 by 57 photogrammetry transects recorded at 13 sites around the island of Moorea (French  
39 Polynesia). Our model was able to predict structural complexity with high accuracy (cross-  
40 validated  $R^2 = 0.81 \pm 0.12$ ). We then used our model to hindcast historical trends in 3D  
41 structural complexity using community composition data collected in Moorea from 2004 to  
42 2017. The temporal analysis highlighted the dramatic effect of a crown-of-thorns outbreak in  
43 2006-2009 and Cyclone Oli in 2010. These two events together reduce coral cover from  $\approx 50\%$   
44 to almost zero. Our model captured these effects, confirming the possibility to predict structural  
45 complexity on the basis of assemblage composition.

## 46 **Introduction**

47           Global concerns are emerging about the increasing frequency of mass mortality of  
48 corals associated to coral bleaching events (Van Oppen and Lough 2009; Heron et al. 2016;  
49 Hughes et al. 2017). These disturbances are associated to severe habitat destruction that reduces  
50 the structural complexity (i.e., flattening) of coral reefs (Newman et al. 2015). Structural  
51 complexity is the three-dimensional spatial arrangement of an ecosystem (McCormick 1994;  
52 Chazdon 2014), which is largely due to the growth form and distribution of hard coral.  
53 According to the habitat heterogeneity hypothesis (MacArthur and Wilson 1967), the more  
54 complex the structure of an ecosystem, the greater the diversity and abundance of associated  
55 organisms. On coral reefs, the 3D structural complexity of the habitat is correlated to the  
56 biomass and diversity of fish (Willis and Anderson 2003; Gratwicke and Speight 2005;  
57 Alvarez-Filip et al. 2009; Rogers et al. 2014), to the reef capacity to recover from disturbance  
58 (Graham et al. 2015), but also to the reef ability to dissipate wave energy, thus protecting the  
59 shoreline from extreme inundations (Harris et al. 2018). Broad-scale declines in the complexity  
60 of coral reefs have been observed both in the Caribbean and the Pacific as a result of both human  
61 impacts and climate changes (Hoegh-Guldberg 1999; Hughes et al. 2003; Hoegh-Guldberg et  
62 al. 2007; Perry et al. 2018). Despite the well-known important relationship between structural  
63 complexity, ecological diversity, abundance and biomass, information on structural complexity  
64 is sparse in monitoring programs with the result that long-term trends for this variable are  
65 virtually unknown (Graham et al. 2015).

66           Methods to measure structural complexity (often referred as rugosity, in particular in  
67 older literature) on coral reefs first arose in the 70' in articles by Risk (1972) and Hobson  
68 (1972). These authors defined three criteria for measuring complexity: 1) the measure had to  
69 be easily understandable, 2) it had to be measurable during the fieldwork and, 3) it should be  
70 comparable. In early studies, it was proposed that rugosity could be recorded by draping a steel  
71 chain over the reef surface, and then measuring the ratio between the total length of the chain

72 and the planar distance between the ends of the chain. The higher the ratio, the more complex  
73 the substratum (Hill and Wilkinson 2004; Graham and Nash 2013). Despite the ease of use of  
74 such metric, laying a chain represents a bi-dimensional measure which does not capture the full  
75 complexity of complex three-dimensional (3D) habitats such as coral reefs. Although some  
76 time-consuming 3D metrics have been proposed in the past (e.g. Parravicini et al. 2006), the  
77 recent progress in underwater photogrammetry are finally affording researchers the opportunity  
78 to capture the three-dimensionality of coral reefs. For example, Friedman et al. (2012) started  
79 to use a georeferenced survey work and each includes a downward-looking camera pair with a  
80 baseline of approximately 7cm, pixel resolution of  $1360 \times 1024$  to define rugosity. Others  
81 authors like Burns et al. (2015) were using these new advances for defining the rugosity about  
82 a transect and extract a complexity index at the species level for 6 species. Leon et al. (2015),  
83 defined three roughness parameters, namely the root means square height, tortuosity (i.e.  
84 rugosity) and fractal dimension, and were derived and compared in order to asses which one  
85 better characterizes reef flat roughness. Naughton et al. (2015) succeed with an accuracy never  
86 equaled to define maps of community structures between taxa. Some writers have even pushed  
87 the boundaries to measure the small-scale three-dimensional features of a shallow-water coral  
88 reef thanks to drone (Casella et al. 2017). Thus, a plethora of works have emerged asking  
89 several authors about the chain-tape future (Storlazzi et al. 2016). However, whatever the metric  
90 employed (chain-tape or photogrammetry methods), there is still no clear evidence concerning  
91 what is driving structural complexity. Some authors claim that it is driven by the presence of  
92 some branching species like the *Acropora* spp. and thus the overall coral cover would not matter  
93 (Aronson and Precht 2006; Alvarez-Filip et al. 2009, 2011). Others have found that coral cover  
94 is significantly and highly correlated to the rugosity (Halford et al. 2004; Graham and Nash  
95 2013) or species composition (Richardson et al. 2017). But in both cases, there is a common  
96 consensus for admitting coral drives complexity which could be used for rebuilding past  
97 rugosities.

98           In this study, we combined statistical modeling to 3D reef transects reconstructed using  
99 photogrammetry in order to test the potential to predict coral reef structural complexity on the  
100 basis of benthic community composition. We study the reefs of Moorea (French Polynesia)  
101 where, using benthic communities time series we back-calculate reef structural complexity. We  
102 were able to retrace two relevant episodes of habitat destruction: the *Acanthaster planci*  
103 outbreak of 2006-2009 and cyclone Oli of 2010.

104

## 105 **Material and Methods**

### 106 **1. Study area**

107           Moorea is a tropical volcanic island of volcanic origin, located in the Pacific Ocean  
108 between 17.4714° and 17.6058° South and 149.7522° and 149.9269° West. The island is  
109 shaped as a triangle with a perimeter of 61 km and coastlines facing north, southwest and  
110 southeast (**Fig. 1**). The island is encircled by a coral reef, that is 500 to 700 m wide; the only  
111 exception to this pattern is the Northeast extremity where the lagoon width is limited to few  
112 tens of meters. Moorea is exposed to Northwest winds from January to March. Tides are  
113 semidiurnal with an amplitude of less than 0.3 m (Chazottes et al. 1995; Leichter et al. 2013).  
114 The swell direction is from southwest to northeast during the whole year.

115           The reefs of Moorea are threatened by several disturbances of biotic and abiotic origin  
116 (Adjeroud et al. 2018). The most devastating biotic disturbances were the 1979 and 2006  
117 *Acanthaster planci* outbreak, which reduced coral cover from 50% to 10% (in 1979; Berumen  
118 and Pratchett 2006) and from 50% to less than 10% (in 2006; Lamy et al. 2016). Abiotic  
119 disturbances also impacted Moorea island, with main cyclones recorded in 1991 (Wasa) and  
120 2010 (Oli). The impact of Wasa reduced the coral cover by 5% to over 20% across all the island.  
121 In contrast, coral cover was reduced to lower than 5% by Cyclone Oli (Lamy et al. 2016;  
122 Adjeroud et al. 2018) (**Fig. 2**).

123

124           **2. Rugosity measures**

125           In Moorea, a total of 57 photogrammetric transects were surveyed in end-of-2015 –  
126 beginning-of-2016, at three different sites: Tiahura (North Coast, 21 transects); Haapiti  
127 (Southwest coast, 20 transects) and Temae (Southeast coast, 16 transects) (**Fig. 1**). Each transect  
128 consisted of swaths of 20m length and 2m width and all transects were carried out in the outer  
129 reef, between 5 and 8m depth. Each transect was set up fixing on the bottom a 2m-long chain  
130 and, perpendicularly to it, a 20m-long metered tape. A diver swam  $\approx 2\text{m}$  above the sea-bottom,  
131 maintaining the swimming speed as constant as possible and collecting images with a GoPro  
132 Hero camera pointed towards the sea-bottom. The camera was set to collect photos (12  
133 megapixels) in time-lapse mode (2 pictures per second). For each transect, we collected  
134 approximately 200 photos with a forward overlap of  $\approx 90\%$ , with the diver swimming over the  
135 length of the entire transect four times to allow optimal side overlap. After the collection of the  
136 photos, the diver noted the depth of each extremity of the chain and metered tape to use them  
137 in the photogrammetric process as Ground Control Points (GCPs). In the case of an on-the-job  
138 self-calibration, the camera calibration is derived from image coordinates measured in the  
139 mapping photography and including the camera calibration parameters as unknowns in a self-  
140 calibrating bundle adjustment (Harwin et al. 2015).

141           The set of photos and the GCPs collected were then used as input to Agisoft Photoscan  
142 ([www.agisoft.com](http://www.agisoft.com)), a photogrammetry software based on the Structure from Motion (SfM)  
143 method (Ullman 1979; Westoby et al. 2012). We used Agisoft to build the orthophotomosaic  
144 and the Digital Elevation Model (DEM) of each transect, with the same procedure explained  
145 by Storlazzi et al. (2016). Details of the photogrammetric process are shown in the **Annex S1**.  
146 Subsequently, we imported the DEM in ArcGIS v10.2 and calculated the reef rugosity by  
147 dividing the surface of the DEM area by the area of its planar projection (approximately  $40\text{m}^2$ )  
148 (**Fig. 3**). For the 57 transects, we estimated an average horizontal error of  $0.1\pm 0.06\text{m}$  and  
149 average vertical error of  $0.04\pm 0.04\text{m}$ , internal to the reconstructed model. Only the vertical error

150 had an influence on the estimation of rugosity, but given the range of the error, it was considered  
151 negligible.

152

### 153 **3. Benthic community description and assessment**

154 The orthophotomosaics were imported into Coral Point Count, which was used  
155 with an Excel extension v4.1 (Kohler and Gill 2006). We assessed the benthic cover placing  
156 100 random points on the photomosaic and described 8 distinct benthic cover categories (**Table**  
157 **1**). A second dataset was used according to the CRIOBE surveys from 2004 to nowadays and  
158 consists of 25m point intercept transects data collected at 13 sites around the island across three  
159 habitats (fringing reef, back reef, outer reef) and using the same benthic categories (**Fig. 1**).  
160 This classification is based on the guideline of the monitoring program created by SO CORAIL  
161 (<http://observatoire.criobe.pf/CRIOBEData/>), the coral reef observation program of the French  
162 National Institute for Earth Sciences and Astronomy (INSU). These categories enabled us to  
163 back-calculate structural complexity on time series data from Moorea. For matching both  
164 datasets according to the habitat, only the outer reef was selected.

165

### 166 **4. Statistical analysis**

167 Our main goal was to calibrate a model that predicts structural complexity according to  
168 the benthic community composition. Since benthic community cover is expressed as  
169 percentages, we preferred not to use them as predictor variables as they are heavily correlated,  
170 and collinearity would have been high. We preferred to build a database that include the time  
171 series data and our photogrammetry transects without transforming the data to perform  
172 multivariate analysis. Thus, the Euclidean distance could be used to conduce a Principal  
173 Component Analyses (PCA). The first five orthogonal axes (accounted for more than 75% of  
174 the variance) were then extracted to be used as predictor variables in the model. A lasso  
175 generalized linear model has been conducted to predict coral reef structural complexity

176 according to the 5 PCA axes. A 10-Fold cross validation was done and a step AIC procedure  
177 defining the best model was applied. Because the 57 transects were measured at the same depth,  
178 those transects were pooled together rather to apply a mixed model due to the lack of the data,  
179 making us benefit from a solid robustness. The best model selected kept only 3 PCA  
180 dimensions. According to the k-fold analysis,  $k R^2$  were obtained giving a necessary uncertainty  
181 for the model. This method appears more meaningful estimate than classical  $R^2$  when the model  
182 has to be used for predictions. The lasso generalized linear model was then applied to time  
183 series data to back-calculate structural complexity and to test whether our model was able to  
184 detect drops of structural complexity due to the major perturbations.

185 The PCA data for the time series in Moorea were used to produce PCA plots and define  
186 the long-term tendencies in order to descriptively assess the entity of the effect of the  
187 *Acanthaster planci* outbreak (2006-2009) and the Oli cyclone (2010) on benthic communities.  
188 An ANOVA was then applied with the aim to define several bunches of similar years according  
189 to the PCA axes. To match those years with each other, a Tukey post-hoc analysis was  
190 conducted and a matrix of results was elaborated. Finally, special attention has been given about  
191 the *Acropora* spp. cover, *Pocillopora* spp. cover and rugosity index in 2004 (pre-disturbance  
192 year, with the high percent cover of corals) and 2017 (post-disturbance year, with the high  
193 percent cover of corals) to define a potential resilience or recovery (**Table S1**).

194

## 195 **Results**

196 The analysis of time series revealed that coral diversity was higher in 2004 with a  
197 percent cover of corals (CC) of 44.08% (**Fig. 4**). The CC decreased from 2004 to 2010 down  
198 to a minimum of 3.62%, which corresponds to the event of Cyclone Oli. After the cyclone  
199 passed, the coral cover increased over time until the end of the series (2017) with a final value  
200 of 42.77%. In 2004 the coral reefs of Moorea also showed a greater diversity of coral  
201 morphology (massive, branching in general, columns and encrusting). The assemblages

202 remained fairly stable despite a slow decline of the CC the first 2 years ( $CC_{2004} = 44.08\%$  to  
203  $CC_{2006} = 40.62\%$ ). Then, a first Crown-Of-Thorns Starfish (COTS) outbreak was reported in  
204 early 2006 (Kayal et al. 2012) and continued until 2009. The following year, cyclone Oli hit the  
205 island further decreasing the CC. After these events and until 2014, the substrate consisted of  
206 rubble and cobbles. From 2015, the CC recovered to a state similar to that of 2004. However,  
207 compared to 2004, the coral cover in 2017 was dominated by *Pocillopora* spp. ( $20.10 \pm 6.78\%$   
208 in 2004 vs  $26.61 \pm 14.52\%$  in 2017) instead of a more diverse assemblage with a high abundance  
209 of *Acropora* spp ( $9.76 \pm 5.61\%$  vs  $2.53 \pm 1.90\%$  in 2017).

210 The cross-validated  $R^2$  (CV- $R^2$ ) from our model reaches  $0.81 \pm 0.12$ . The 3 dimensions  
211 used were all significant and non-correlate (**Table 2, Fig S1**). The back calculation of structural  
212 complexity captured these major shifts in community structure. High structural complexity was  
213 observed in 2005 and 2006. All sites were then predicted to lose complexity corresponding to  
214 the timing of COTS outbreak models present patterns of decrease and increase in rugosity,  
215 matching with the biotic and abiotic changes like the COTS outbreak and the Cyclone Oli, as  
216 discussed above (**Fig. 5**). The model also exemplifies that the resilience of structural  
217 complexity differs among the thirteen reefs studied around Moorea island. In 2004, the  
218 highest values of structural complexity were measured respectively at Pihaena (North),  
219 Motu Ahi (East) and Haapiti (Northwest) (3.86, 3.51 and 2.92 respectively) while the  
220 lowest were recorded in Maatea (Southeast), Tiahura (North) and Aroa (North) (2.26,  
221 2.07 and 1.81 respectively). After the disturbances in 2010, the higher values were  
222 defined in Taotaha (Northwest), Afareaitu (Southeast) and Entre 2 Baies (North) (2.08,  
223 2.10 and 2.10 respectively) while the lowest values were documented at Haapiti  
224 (Northwest), Tiahura (North) and Maatea (Southeast) (1.84, 1.66 and 1.15 respectively).  
225 Finally, in 2017, the 3 lowest values were measured on the East coast (Motu Ahi, Maatea  
226 and Temae with rugosity values of 2.35, 2.12 and 1.98 respectively) while the sites located

227 on the northwest side (Entre 2 Baies, Tiahura and Gendron) presented the 3 higher  
228 rugosity scores (4.36, 4.31 and 3.53 respectively).

229 Finally, rugosity values rise to values equivalent to the first year of monitoring, during  
230 the last year of monitoring in 2017. The presence of *Acropora* spp. shows a significant  
231 difference between 2004 and 2017. However, no significant difference could be observed in  
232 either the *Pocillopora* spp. presence or the rugosity score (**Fig. 6**). In addition, the ANOVA  
233 followed by the post-hoc analysis confirmed a difference between two bunches of years  
234 according to the complexity around the island. Indeed, two profiles were highlighted: 1)  
235 one from 2004 to 2007 and 2016 to 2017 and 2) one from 2008 to 2015. These results  
236 support that the 3D complexity came back to an equilibrium four years after the Oli  
237 cyclone (**Table S1**).

238

## 239 **Discussion**

240 In this study we used a combination of methods – coral reef photogrammetry and  
241 statistical models – to test the potential to use species composition data to predict the structural  
242 complexity of coral reef assemblages. The use of the photogrammetry allowed us to obtain a  
243 three-dimensional metric of structural complexity, compared to linear metrics classically used  
244 such as the chain transect (Burns et al. 2015). Photogrammetry permits us to cover 40m<sup>2</sup> of the  
245 reef in one dive of about 90 minutes, whereas the chain method usually requires  
246 approximatively 15 minutes for a simple 20m transect. However, even if the pixel size of 1.73  
247 × 1.73 μm - used for defining the complexity - is higher resolution than what is achieved using  
248 chain and tape, the results have to be interpreted with cautious. Indeed, a number of studies  
249 have shown photogrammetry to be error prone in a number of different ways. Lavy et al. (2015)  
250 and Figueira et al. (2015) both found that branching corals and other complex growth forms  
251 produce more error in photogrammetry-based estimates of complexity compared to in situ  
252 methods. Furthermore, Bryson et al. (2017) found that environmental conditions,

253 postprocessing, and even taking photos underwater can impact the accuracy of 3D structure  
254 estimates using photogrammetry. In addition, this model is relevant for planar parts of the  
255 reef, however, facing dropoff would be challenging. This technique requires swimming  
256 over the bottom, nevertheless, as the more the distance you add between you and the  
257 bottom, the worst the reconstruction will be. Finally, all the hidden part (not present in  
258 the photos) are not reconstructed (e.g. what is inside a hole). The latter limit causes  
259 relatively heavy consequences to define an accurate measure of the rugosity in those  
260 conditions. From a statistical point of view, Carroll et al. (2006) defined 3 different regimes of  
261 swell in Moorea which could altered the benthic composition, according to the exposure due to  
262 the side of the island. Even if these affirmations are directly observable concerning the rugosity  
263 in 2017 with our current model (lowest values on the east coast and higher values on the north  
264 coast) a mixed model would have been more relevant. Unfortunately, only 16 transects were  
265 done on the southeast side of Moorea which is not allowed us for using a mixed model. The  
266 robustness of the model would have been directly impacted by the lack of residuals (rugosity  
267 values sometimes lower than 1; Launer & Wilkinson, 2014). As per any statistical model, the  
268 accuracy of prediction will increase with the size of the calibrating dataset. In that context, more  
269 data will likely be needed to accurately capture spatial variation.

270         Despite these limits, we have found a significant relationship between reef structural  
271 complexity and the composition of the benthic assemblages. Indeed 3 PCA axes were enough  
272 to accurately predict complexity with a high accuracy ( $CV-R^2 = 0.81 \pm 0.12$ ). To validate our  
273 model, we compared our values to (Kayal et al. 2017). These authors have found values at 12m-  
274 depth of  $1.44 \pm 0.08$ ,  $1.41 \pm 0.05$  and  $1.70 \pm 0.03$  for Haapiti, Tiahura and Entre 2 Baies  
275 respectively. Our model suggests values for these locations of  $1.75 \pm 0.50$ ,  $1.68 \pm 0.47$  and  $1.70$   
276  $\pm 0.60$  respectively. Thus, even according the huge range of the uncertainties, our results  
277 highlight the potential to use statistical modeling to predict structural complexity when this  
278 information is lacking. Given the importance of structural complexity in ecological functioning

279 of coral reefs, the reconstruction of structural complexity is critical from long-term benthic  
280 historical data, if we want to better understand and predict changes in coral reefs. For example,  
281 Graham and Nash (2013) reviewed 20 studies using chain method to measure coral reef rugosity  
282 in the Caribbean and found a strong negative relationship between structural complexity and  
283 algal cover, a positive relationship between the structural complexity and the coral cover, and  
284 a strong positive relationship between structural complexity and fish density and biomass.  
285 Later, Graham et al. (2015) demonstrated that structural complexity is the main predictor of  
286 coral reef recovery capacity after acute disturbance. This metric represents thus a key variable  
287 of coral reef status, and apodictically exists also regarding the present day flattening of coral  
288 reefs under the influence of climate change and human impacts. Back-calculating structural  
289 complexity, with due caution, may be important to infer present coral reef status compared to  
290 historical or quasi-pristine conditions.

291 Here, we have documented major changes in benthic assemblages across Moorea's coral  
292 reefs (Berumen and Pratchett 2006; Adjeroud et al. 2018). *Acropora* spp. and *Pocillopora* spp.  
293 were dominant species in 2003 (Berumen and Pratchett 2006) and this was still the case in 2004.  
294 *Pocillopora* spp. then, *Acropora* spp. were affected by both COTS outbreak and the Oli cyclone  
295 more than any other taxon (Kayal et al. 2012). Branching and table-shaped species belonging  
296 to the genus *Acropora* were affected first and most heavily. Then, it was followed by those of  
297 sub-branching *Pocillopora*. Finally, Populations of encrusting *Montipora*, massive *Porites*, and  
298 other hard-coral assemblages also declined, showing a synchronized collapse with the entire  
299 coral communities. From 2011 onward, benthic assemblages started to recover mainly thanks  
300 to encrusting coral forms and *Pocillopora* spp. that is presently the dominating coral form in  
301 Moorea. The current *Pocillopora*-dominated state may be a transitional phase, indicative of  
302 either continuing degradation or recovery (Aronson et al. 2004). Our back-calculated structural  
303 complexity was able to capture major changes due to COTS outbreak and Cyclone Oli, thus  
304 attesting the potential to use statistical modeling when the rugosity has not been empirically

305 collected. However, the status of coral reefs in 2004 when *Acropora* spp. was on average  $\approx 10\%$   
306 and the present status (average *Acropora* cover  $\approx 2\%$ ) was not enough to distinguish difference  
307 in back-calculated structural complexity. There are two proposed explanations for this  
308 observation: (a) our model is calibrated with present-day data. Only two transects in 2017 had  
309 assemblages with an *Acropora* cover higher than 5% which is a consequent statistic assumption  
310 according to the *Acropora* cover in 2004 ( $9.76 \pm 5.61\%$  in 2004 vs  $2.53 \pm 1.90\%$  in 2017). This  
311 again results in an extremely cautious interpretation of the results due to a possible  
312 underestimation of *Acropora* spp. in the past years (Aronson and Precht 2006; Alvarez-Filip et  
313 al. 2009, 2011). And/or (b) *Acropora* and *Pocillopora* taxa harbored branching form and  
314 similarly contribute to the complexity (Reichert et al. 2017). Thus, the complexity could be  
315 rebuilt according to the coral cover underlying the different coral morphologies (Halford et al.  
316 2004; Graham and Nash 2013; Richardson et al. 2017). In order to sharp our hindcasting, the  
317 reproducibility of this method could allow us to find a new area with the needed information  
318 (i.e. past *Acropora* and *Pocillopora* cover vs post *Acropora* and *Pocillopora* cover and past and  
319 post rugosity) and to test our model. Waiting for this improvement, the CC could be enough  
320 accurate to rebuild the past and to predict the complexity for the coming years. Indeed, today  
321 more than ever, global coral reefs are witnessing the effects of climate changes, local impacts  
322 and natural stressors. Coral bleaching is affecting global coral reefs with an unprecedented  
323 frequency and intensity and the future structural complexity of coral reefs is expected to be  
324 reduced by these repeated perturbations (Hughes et al. 2018; Lough et al. 2018). As a  
325 consequence a loss of ecological diversity productivity is likely (Alvarez-Filip et al. 2009).

326

327

328

329

330

331

332

333 **Conflict of interest:** On behalf of all authors, the corresponding author states that there  
334 is no conflict of interest.

335 **References**

- 336
- 337 Adjeroud M, Vercelloni J, Bosserelle P, Chancerelle Y, Kayal M, Iborra-Cantonnet C, Penin  
338 L, Liao V, Claudet J (2018) Recovery of coral assemblages despite acute and recurrent  
339 disturbances on a South Central Pacific reef. *Sci Rep* 8:8
- 340 Alvarez-Filip L, Côté IM, Gill JA, Watkinson AR, Dulvy NK (2011) Region-wide temporal  
341 and spatial variation in Caribbean reef architecture: Is coral cover the whole story? *Glob*  
342 *Chang Biol* 17:2470–2477
- 343 Alvarez-Filip L, Dulvy NK, Gill JA, Côté IM, Watkinson AR (2009) Flattening of Caribbean  
344 coral reefs: Region-wide declines in architectural complexity. *Proc R Soc B Biol Sci*  
345 276:3019–3025
- 346 Aronson RB, MacIntyre IG, Wapnick CM, O’Neill MW (2004) Phase shifts alternative states  
347 and the unprecedented convergence of two reef systems. *Ecol Soc Am* 85:1876–1891
- 348 Aronson RB, Precht WF (2006) Conservation, precaution, and Caribbean reefs. *Coral Reefs*  
349 25:441–450
- 350 Berumen ML, Pratchett MS (2006) Recovery without resilience: Persistent disturbance and  
351 long-term shifts in the structure of fish and coral communities at Tiahura Reef, Moorea.  
352 *Coral Reefs* 25:647–653
- 353 Bryson M, Ferrari R, Figueira W, Pizarro O, Madin J, Williams S, Byrne M (2017)  
354 Characterization of measurement errors using structure-motion and photogrammetry to  
355 measure marine habitat structural complexity. *Ecol Evol* 7:5669–5681
- 356 Burns J, Delparte D, Gates R, Takabayashi M (2015) Integrating structure-from-motion  
357 photogrammetry with geospatial software as a novel technique for quantifying 3D  
358 ecological characteristics of coral reefs. *PeerJ* 3:19
- 359 Carroll A, Harrison P, Adjeroud M (2006) Sexual reproduction of *Acropora* reef corals at  
360 Moorea , French Polynesia. *Coral Reefs* 25:93–97
- 361 Casella E, Collin A, Harris D, Ferse S, Bejarano S, Parravicini V, Hench JL, Rovere A (2017)  
362 Mapping coral reefs using consumer-grade drones and structure from motion  
363 photogrammetry techniques. *Coral Reefs* 36:269–275
- 364 Chazdon RL (2014) Second Growth, the promise of tropical forest regeneration in an age of  
365 deforestation.
- 366 Chazottes V, Le Campion-Alsumard T, Peyrot-Clausade M (1995) Bioerosion rates on coral  
367 reefs : interactions between macroborers , \* Experimental site. *Palaeogeogr Palaeoclimatol*  
368 *Palaeoecol* 113:189–198
- 369 Figueira W, Ferrari R, Weatherby E, Porter A, Hawes S, Byrne M (2015) Accuracy and  
370 Precision of Habitat Structural Complexity Metrics Derived from Underwater  
371 Photogrammetry. *Remote Sens* 7:16883–16900
- 372 Friedman A, Pizarro O, Williams SB, Johnson-Roberson M (2012) Multi-Scale Measures of  
373 Rugosity, Slope and Aspect from Benthic Stereo Image Reconstructions. *PLoS One* 7:14
- 374 Graham NAJ, Jennings S, MacNeil MA, Mouillot D, Wilson SK (2015) Predicting climate-  
375 driven regime shifts versus rebound potential in coral reefs. *Nature* 518:7
- 376 Graham NAJ, Nash KL (2013) The importance of structural complexity in coral reef  
377 ecosystems. *Coral Reefs* 32:315–326
- 378 Gratwicke B, Speight MR (2005) Effects of habitat complexity on Caribbean marine fish  
379 assemblages. *Mar Ecol Prog Ser* 292:301–310
- 380 Halford A, Cheal AJ, Ryan D, Williams DM (2004) Resilience to Large-Scale Disturbance in  
381 Coral and Fish Assemblages on the Great Barrier Reef. *Ecol Soc Am* 85:1892–1905
- 382 Harris DL, Pomeroy A, Power H, Casella E, Rovere A, Webster JM, Parravicini V, Canavesio  
383 R, Collin A (2018) Coral reef structural complexity provides important coastal protection  
384 from waves under rising sea levels. *Sci Adv* 4:7
- 385 Harwin S, Lucieer A, Osborn J (2015) The Impact of the Calibration Method on the Accuracy  
386 of Point Clouds Derived Using Unmanned Aerial Vehicle Multi-View Stereopsis. *Remote*

387 Sens 7:11933–11953

388 Heron SF, Maynard JA, Van Hooidek R, Eakin CM (2016) Warming Trends and Bleaching  
389 Stress of the World’s Coral Reefs 1985-2012. *Sci Rep* 6:14

390 Hill J, Wilkinson C (2004) Methods for ecological monitoring of coral reefs: A resource for  
391 managers. Version 1. Australian Institute of Marine Science, Townsville, 117.

392 Hobson RD (1972) Surface Roughness in Topography: A Quantitative Approach. *Spatial*  
393 *Analysis in Geomorphology* 221-245

394 Hoegh-Guldberg O (1999) Climate Change, coral bleaching and the future of the world’ s coral  
395 reefs. *Mar Freshw Res* 50:839–866

396 Hoegh-Guldberg O, Mumby PJ, Hooten AJ, Steneck RS, Greenfield P, Gomez E, Harvell CD,  
397 Sale PF, Edwards AJ, Caldeira K, Knowlton N, Eakin CM, Iglesias-Prieto R, Muthiga N,  
398 Bradbury RH, Dubi A, Hatziolos ME (2007) Coral reefs under rapid climate change and  
399 ocean acidification. *Science* (80- ) 318:1737–1742

400 Hughes TP, Álvarez-Noriega M, Álvarez-Nomero JG, Anderson KD, Baird AH, Babcock RC,  
401 Beger M, Bellwood DR, Berkelmans R, Bridge TC, Butler IR, Byrne M, Cantin NE,  
402 Comeau S, Connolly SR, Cumming GS, Dalton SJ, Kerry JT, Kuo C, Lough JM, Hoey  
403 AS, Hobbs JA, Hoogenboom MO, Emma V, Pears RJ, Pratchett MS, Schoepf V, Simpson  
404 T, Skirving WJ, Sommer B (2017) Global warming and recurrent mass bleaching of corals.  
405 *Nature* 543:373–377

406 Hughes TP, Anderson KD, Connolly SR, Heron SF, Kerry JT, Lough JM, Baird AH, Baum JK,  
407 Berumen ML, Bridge TC, Claar DC, Eakin CM, Gilmour JP, Graham NAJ, Harrison H,  
408 Hobbs JA, Hoey AS, Hoogenboom M, Lowe RJ, Mcculloch MT, Pandolfi JM, Pratchett  
409 M, Schoepf V (2018) Spatial and temporal patterns of mass bleaching of corals in the  
410 Anthropocene. *Science* (80- ) 83:80–83

411 Hughes TP, Baird AH, Bellwood DR, Card M, Connolly SR, Folke C, Grosberg R, O. H-G,  
412 Jackson JBC, Kleypas J, Lough JM, Marshall P, Nyström M, Palumbi SR, Pandolfi JM,  
413 Rosen B, Roughgarden J (2003) Climate Change, Human Impacts, and the Resilience of  
414 Coral Reefs. *Science* (80- ) 301:929–933

415 Kayal M, Bosserelle P, Adjeroud M (2017) Bias associated with the detectability of the coral-  
416 eating pest crown-of-thorns seastar and implications for reef management Subject  
417 Category : Subject Areas : *R Soc Open Sci* 4(8), 170396.

418 Kayal M, Vercelloni J, Lison de Loma T, Bosserelle P, Chancerelle Y, Geoffroy S, Stievenart  
419 C, Michonneau F, Penin L, Planes S, Adjeroud M (2012) Predator Crown-of-Thorns  
420 Starfish (*Acanthaster planci*) Outbreak, Mass Mortality of Corals, and Cascading Effects  
421 on Reef Fish and Benthic Communities. *PLoS One* 7(10), e47363.

422 Kohler KE, Gill SM (2006) Coral Point Count with Excel extensions (CPCe): A Visual Basic  
423 program for the determination of coral and substrate coverage using random point count  
424 methodology. *Comput Geosci* 32:1259–1269

425 Lamy T, Galzin R, Kulbicki M, Lison de Loma T, Claudet J (2016) Three decades of recurrent  
426 declines and recoveries in corals belie ongoing change in fish assemblages. *Coral Reefs*  
427 35:293–302

428 Launer RL, & Wilkinson GN (2014) *Robustness in statistics*. Academic Press.

429 Lavy A, Eyal G, Neal B, Keren R, Loya Y, Ilan M (2015) A quick , easy and non-intrusive  
430 method for underwater volume and surface area evaluation of benthic organisms by 3D  
431 computer modelling. *Methods Ecol Evol* 6:521–531

432 Leichter JJ, Alldredge AL, Bernardi G, Brooks AJ, Carlson CA, Carpenter RC, Edmunds J,  
433 Fewings, M. R, Hanson, K. M, Hench, J. L, Holbrook J, Nelson, G. E, Schmitt, R. J,  
434 Toonen, R. J, Washburn L, Wyatt, S. J (2013) Biological and physical interactions on a  
435 tropical island coral reef: transport, and retention processes on Moorea, French Polynesia.  
436 *Oceanography* 26:52–63

437 Leon JX, Roelfsema CM, Saunders MI, Phinn SR (2015) Measuring coral reef terrain  
438 roughness using “Structure-from-Motion” close-range photogrammetry. *Geomorphology*

439 242:21–28

440 Lough JM, Anderson KD, Hughes TP (2018) Increasing thermal stress for tropical coral reefs :  
441 1871 – 2017. *Sci Rep* 1–8

442 MacArthur RH, Wilson EO (1967) *The Theory of Island Biogeography*.

443 McCormick MI (1994) Comparison of field methods for measuring surface tomography and  
444 their associations with a tropical reef fish assemblage. *Mar Ecol Prog Ser* 112:87–96

445 Naughton P, Kastner R, Sandin S, Kuester F, Edwards C, Petrovic V (2015) Scaling the  
446 Annotation of Subtidal Marine Habitats. *Proc 10th Int Conf Underw Networks Syst* 1–5

447 Newman SP, Meesters EH, Dryden CS, Williams SM, Sanchez C, Mumby PJ, Polunin NVC  
448 (2015) Reef flattening effects on total richness and species responses in the Caribbean. *J*  
449 *Anim Ecol* 84:1678–1689

450 Van Oppen MJH, Lough JM (2009) Coral Bleaching Patterns, Processes, Causes and  
451 Consequences.

452 Parravicini V, Rovere A, Donato M, Morri C, Bianchi CN (2006) A method to measure three-  
453 dimensional substratum rugosity for ecological studies: an example from the date-mussel  
454 fishery desertification in the north-western Mediterranean. *J Mar Biol Assoc United*  
455 *Kingdom* 86:689–690

456 Perry CT, Alvarez-Filip L, Graham NAJ, Mumby PJ, Wilson SK, Kench PS, Manzello DP,  
457 Morgan KM, Slangen ABA, Thomson DP, Januchowski-Hartley F, Smithers SG, Steneck  
458 RS, Carlton R, Edinger EN, Enochs IC, Estrada-Saldívar N, Haywood MDE, Kolodziej  
459 G, Murphy GN, Pérez-Cervantes E, Suchley A, Valentino L, Boenish R, Wilson M,  
460 Macdonald C (2018) Loss of coral reef growth capacity to track future increases in sea  
461 level. *Nature* 558:396–400

462 Reichert J, Backes AR, Schubert P, & Wilke T (2017) The power of 3D fractal dimensions for  
463 comparative shape and structural complexity analyses of irregularly shaped organisms.  
464 *Methods in Ecology and Evolution*, 8(12), 1650-1658.

465 Richardson LE, Graham NAJ, Hoey AS (2017) Cross-scale habitat structure driven by coral  
466 species composition on tropical reefs. *Sci Rep* 7:11

467 Risk MJ (1972) Fish diversity on a coral reef in the virgin islands. *Atoll Res Bull*

468 Rogers A, Blanchard JL, Mumby PJ (2014) Vulnerability of coral reef fisheries to a loss of  
469 structural complexity. *Curr Biol* 24:1000–1005

470 Storlazzi CD, Dartnell P, Hatcher GA, Gibbs AE (2016) End of the chain? Rugosity and fine-  
471 scale bathymetry from existing underwater digital imagery using structure-from-motion  
472 (SfM) technology. *Coral Reefs* 35:889–894

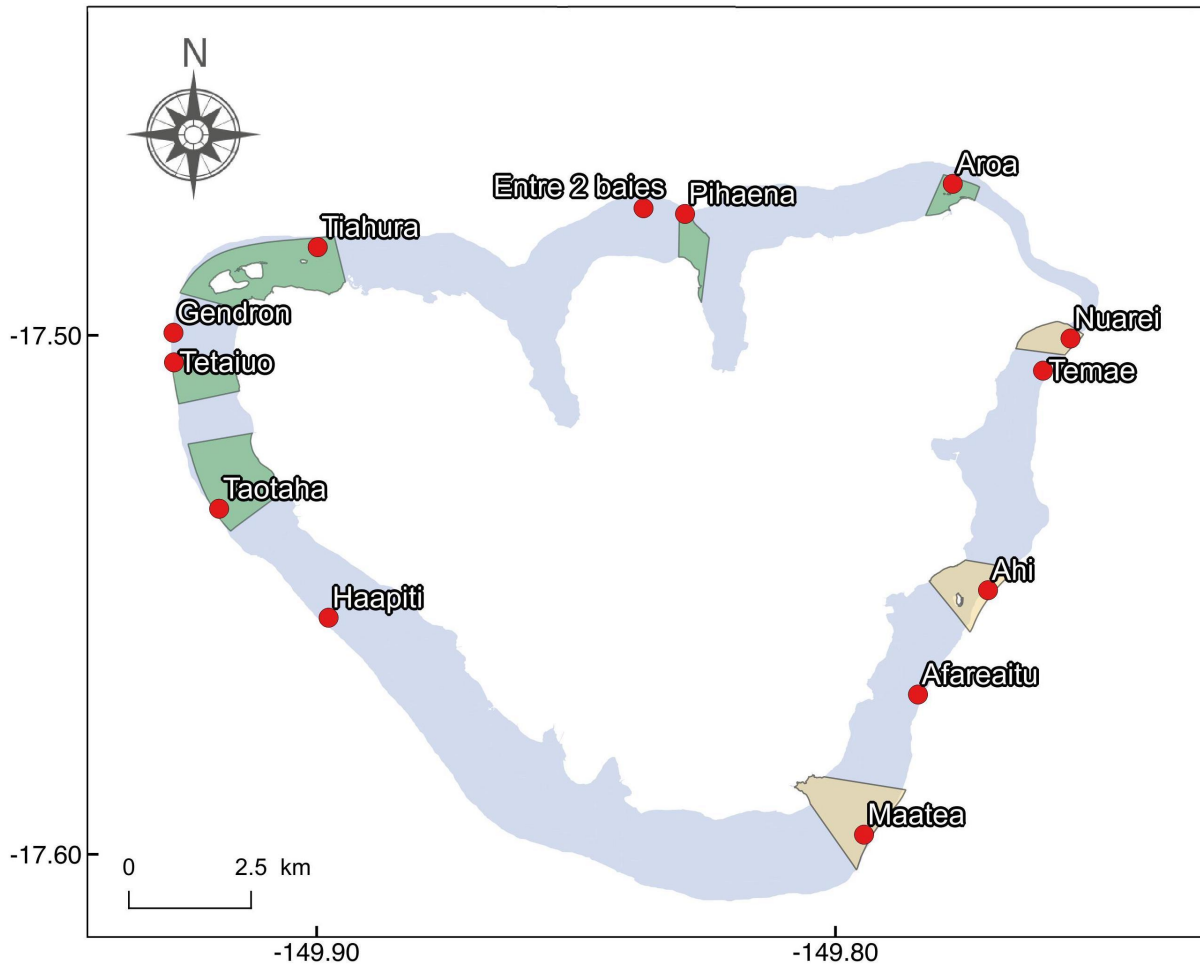
473 Ullman S (1979) The interpretation of structure from motion. *Proc R Soc Lond B Biol Sci*  
474 203:405–426

475 Westoby MJ, Brasington J, Glasser NF, Hambrey MJ, Reynolds JM (2012) “Structure-from-  
476 Motion” photogrammetry: A low-cost, effective tool for geoscience applications.  
477 *Geomorphology* 179:300–314

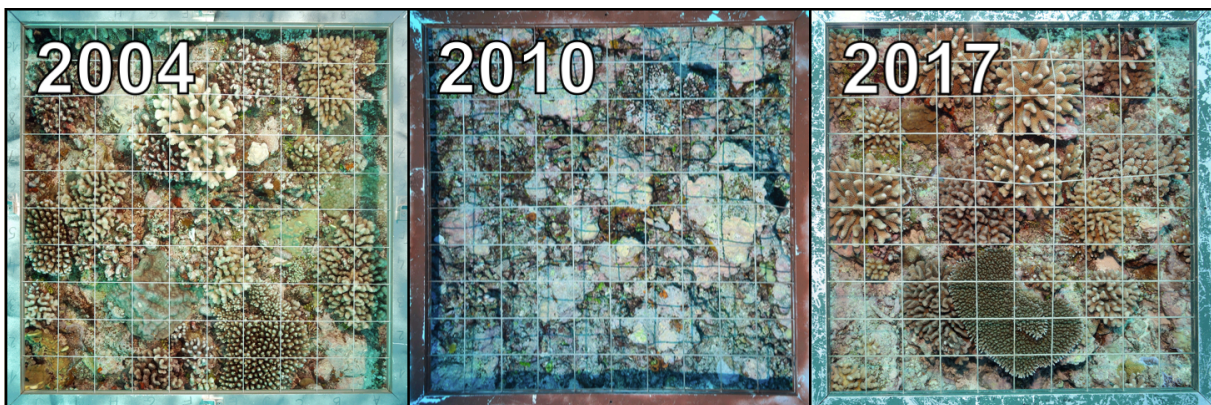
478 Willis TJ, Anderson MJ (2003) Structure of cryptic reef fish assemblages: relationships with  
479 habitat characteristics and predator density. *Mar Ecol Prog Ser* 257:209–221

480

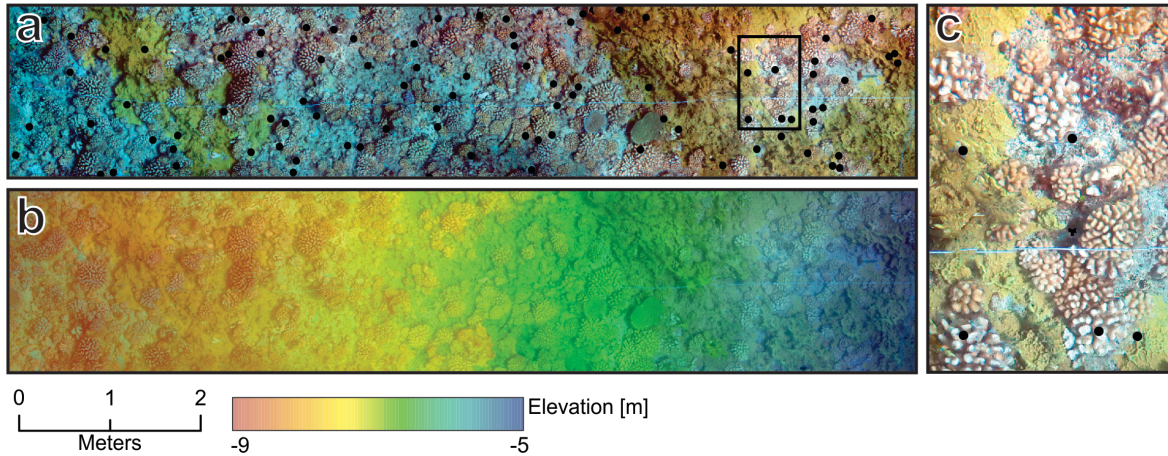
481



484  
485 **Fig. 1** Location of the 13 sites sampled each year since 2004 from 2017 of the MPA monitoring  
486 (red dots) around the island of Moorea. The 5 fully protected MPAs are highlighted in green  
487 and the restricted MPAs are highlighted in yellow. The 5 sites outside of the MPAs are controls.  
488

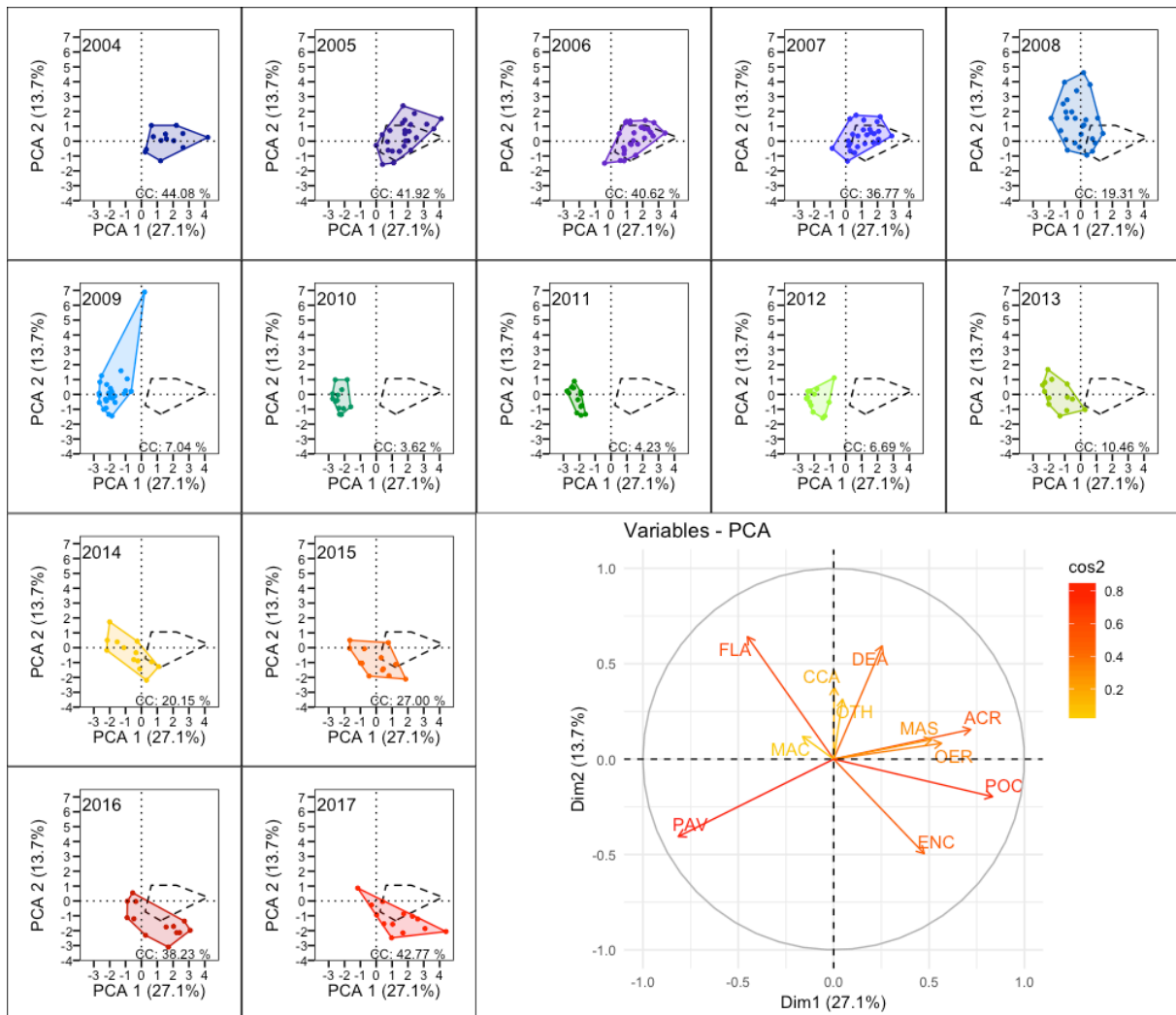


489  
490 **Fig. 2** Evolution of one of the twenty quadrats used to define the coral cover in Haapiti (South  
491 West of the island) before (in 2004), during (in 2010) and after (in 2017) Cyclone Oli.  
492  
493  
494  
495  
496  
497



498  
499  
500  
501  
502  
503  
504

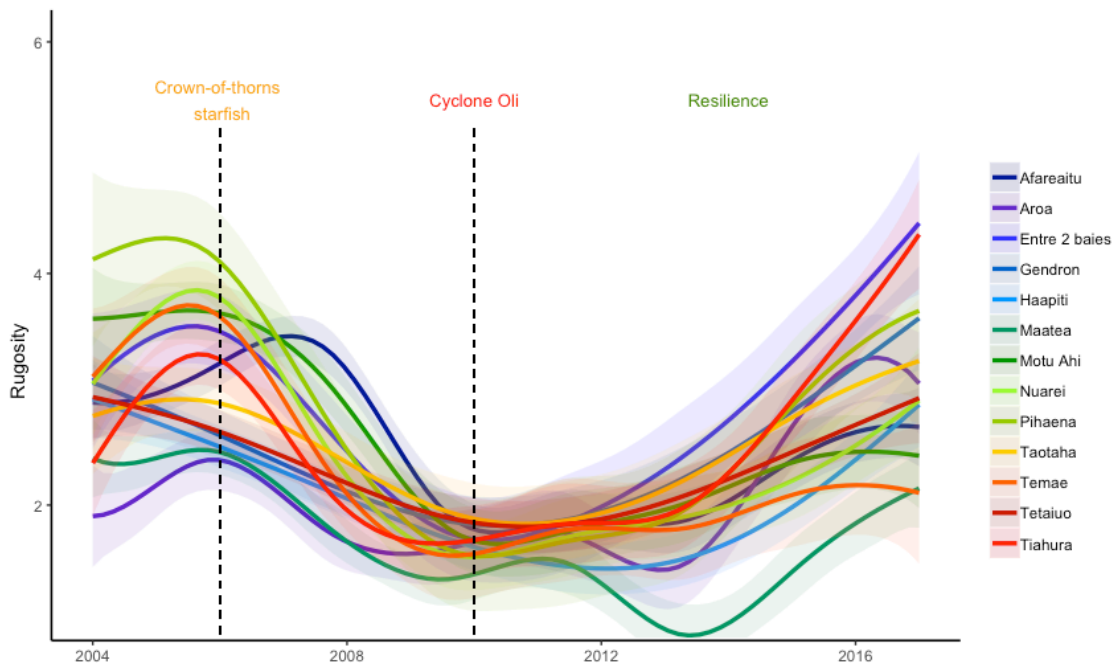
**Fig. 3** Example of results from underwater photogrammetry. a) Orthorectified photomosaic. The black dots indicate the random points where the shape classification has been carried out. b) Digital Elevation Model representing depth values (the photomosaic is kept in transparency in the background). c) Detail of the photomosaic.



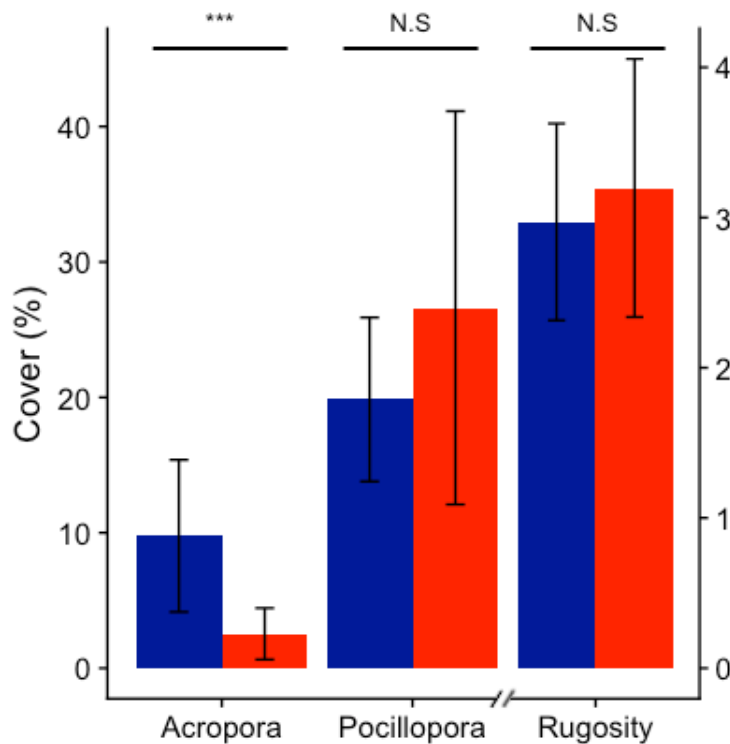
505  
506  
507  
508  
509

**Fig. 4** Principal Components Analysis (PCA) using the 11 morpho-species respecting the code as follows: ACR - Acropora spp; CCA - Crustose Coralline Algae; DEA - Dead Coral; ENC - Encrusting Corals; FLA - Flat (Sand or Mud); MAC - Macroalgae; MAS - Massive corals; OER

510 - Other Erects Forms; OTH - Others (Sponges or benthic species); PAV - Pavement; and POC  
 511 - Pocillopora spp. The PCA was used year by year from 2004 to 2017 and the coral cover (CC)  
 512 is written at the bottom right of each box. The coral community in 2004 is referred as model in  
 513 black dashed lines each year.



514  
 515 **Fig. 5** Rugosity reconstruction from 2004 to 2017 according to the average model and according  
 516 to the 13 sites around the island of Moorea. Both biologic invasion and extreme climatic  
 517 weather events are shown for respectively 2006 and 2010.  
 518



519  
 520 **Fig. 6** Difference between the Acropora and the Pocillopora cover (%) on the left, and the  
 521 difference in rugosity (index) on the right. The dark blue color represents 2004 instead of 2017  
 522 is representing in red. The p-value is represented on the top of each barplot according to the

523 significant R code (\*\*\* highly significant (<0.001), \*\*very significant (<0.01), \* significant  
 524 (<0.05), . almost significant (<0.1), N.S non-significant; threshold: p-value = 0.05)  
 525

526 **Tab. 1** Categories of shape classification defined and used to rebuild the rugosity these last 14  
 527 years. 9 variables are morphologic instead a distinction at the genus level is done for *Acropora*  
 528 spp. and *Pocillopora* spp. The CCA was differentiated from the pavement according to their  
 529 extension: when this later was higher than 100 cm<sup>2</sup>, which corresponds to a projected surface  
 530 of a circle of radius of 5-6 cm it was considered as CCA rather than pavement. The dead corals  
 531 category understands rubbles and cobbles. The flattening category represents sand or mud  
 532 substrate. The categories Encrusting, Other Erect Forms and Massive represent different coral  
 533 morphologies. Finally, the others category represents mostly benthic organism like echinoid or  
 534 even sponges.  
 535

---

<b>ACR</b>	<i>Acropora</i> spp.
<b>CCA</b>	Coralline Crustose Algae
<b>DEA</b>	Dead corals
<b>ENC</b>	Encrusting corals
<b>FLA</b>	Flat (Mud, Sand)
<b>MAC</b>	Macroalgae
<b>MAS</b>	Massive corals
<b>OER</b>	Corals with other erects forms
<b>OTH</b>	Other (like echinoid)
<b>PAV</b>	Pavement
<b>POC</b>	<i>Pocillopora</i> spp.

---

536  
 537 **Tab. 2** Coefficients and standard error for each parameter according to best model defined:  
 538 **Rugosity ~ Dim 1 + Dim 3 + Dim 5** (AIC = 71.776 and R<sup>2</sup> = 0.81 ± 0.12). The p-value  
 539 represents the significance of each parameters according to the R code (\*\*\* highly significant  
 540 (<0.001), \*\*very significant (<0.01), \* significant (<0.05), . almost significant (<0.1), N.S non-  
 541 significant; threshold: p-value = 0.05)  
 542

---

	<b>Estimate</b>	<b>Standard Error</b>	<b>p-value</b>
<b>Intercept</b>	1.65970	0.14616	1.08e-15 (***)
<b>Dimension 1</b>	0.53283	0.08602	9.48e-08 (***)
<b>Dimension 3</b>	0.41917	0.07003	2.03e-07 (***)
<b>Dimension 5</b>	-0.15003	0.06090	1.71e-02 (*)

---

543  
 544

545 **Appendix**

546

547 **Tab. S1** Post Hoc (Tukey HSD) matrix for testing the rugosity difference according to each  
 548 year combination. The P-value (threshold: 0.05) for each combination is written in the matrix  
 549 data as follows. The red values are significantly different and the blue values are not.

550

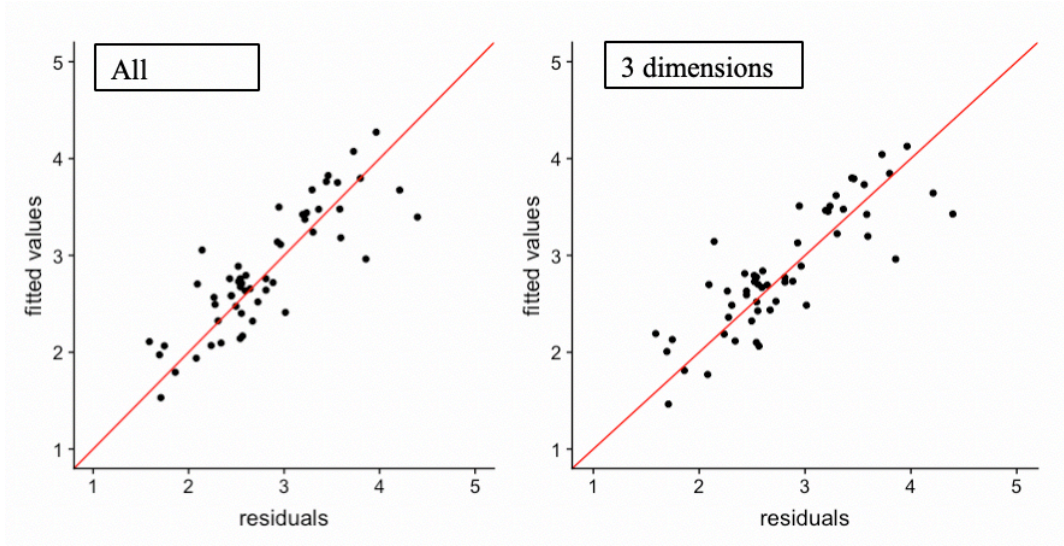
	2004	2005	2006	2007	2008	2009	2010	2011	2012	2013	2014	2015	2016	2017
2004	1.00													
2005	0.98	1.00												
2006	0.96	1.00	1.00											
2007	1.00	0.87	0.80	1.00										
2008	0.04	0.00	0.00	0.00	1.00									
2009	0.00	0.00	0.00	0.00	0.93	1.00								
2010	0.00	0.00	0.00	0.00	0.96	1.00	1.00							
2011	0.00	0.00	0.00	0.00	0.95	1.00	1.00	1.00						
2012	0.00	0.00	0.00	0.00	0.98	1.00	1.00	1.00	1.00					
2013	0.01	0.00	0.00	0.00	1.00	1.00	1.00	1.00	1.00	1.00				
2014	0.11	0.00	0.00	0.03	1.00	1.00	0.99	0.99	1.00	1.00	1.00			
2015	0.91	0.05	0.04	0.81	1.00	0.20	0.31	0.30	0.35	0.51	0.98	1.00		
2016	1.00	1.00	0.99	1.00	0.01	0.00	0.00	0.00	0.00	0.00	0.05	0.80	1.00	
2017	1.00	1.00	1.00	1.00	0.00	0.00	0.00	0.00	0.00	0.00	0.00	0.34	1.00	1.00

551

552

553 **Fig. S1** Analysis of the residuals (fitted values vs observations) from the total model: Rugosity  
 554 ~ Dim 1 + Dim 2 + Dim 3 + Dim 4 + Dim 5 (AIC = 71.8,  $R^2 = 0.78 \pm 0.08$ ) on the left and the  
 555 best model Rugosity ~ Dim 1 + Dim 3 + Dim 5 (AIC = 73.6,  $R^2 = 0.81 \pm 0.12$ ) on the right.

556



557

558

559 **Annex**

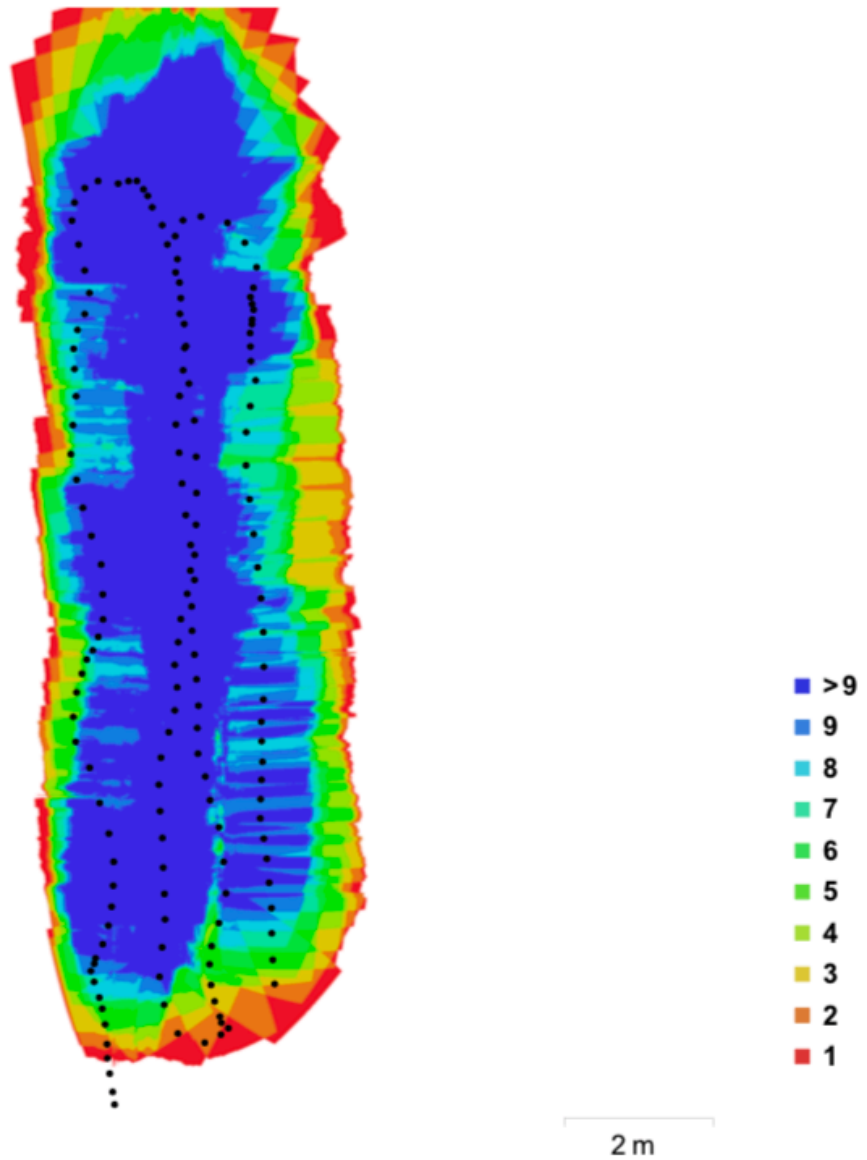
560

561 **Annex S1** Report from Agisoft Photoscan for one site, detailing the settings used for the  
 562 processing of underwater photos.

563

564 **1. Survey Data**

565



566

567 **Fig. 1** Camera locations and image overlap

568

Number of images:	157	Camera stations:	157
Flying attitude:	2.56m	Tie points:	139.838
Ground resolution:	0.53 mm/pix	Projections:	383.598
Coverage area:	56.3 sq m	Reprojection error:	1.88 pix

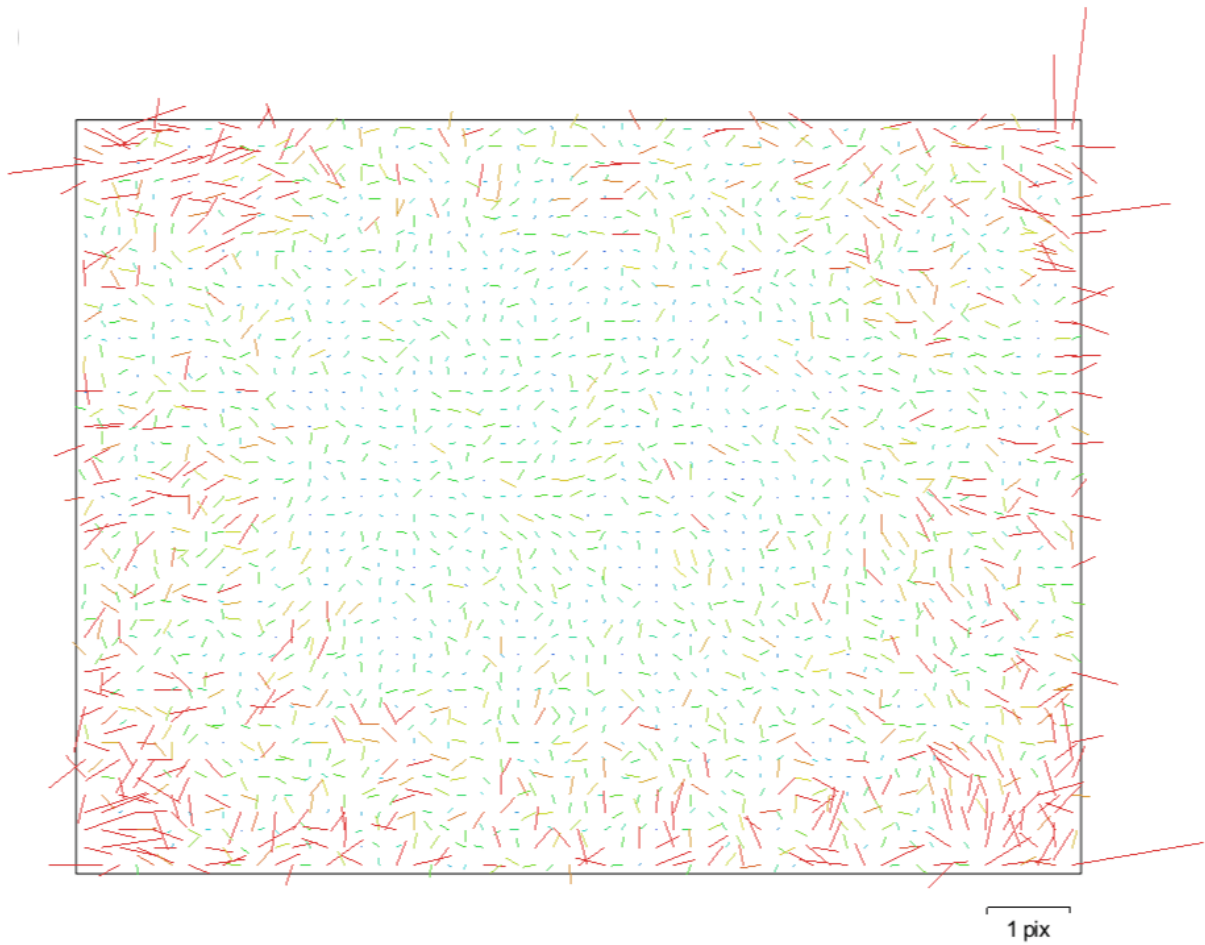
569

570 **Tab. 1** Cameras

Camera Model	Resolution	Focal Length	Pixel Size
HERO4 Black (3 mm)	4000 x 3000	3mm	1.73 x 1.73 um

571

572 **2. Camera calibration**



574 **Fig. 2** Image residuals for HERO4 Black (3 mm).  
 575

576  
 577  
 578

**HERO4 Black (3mm)**

157 images

Resolution <b>4000x3000</b>	Focal length <b>3 mm</b>	Pixel size <b>1.73 x 1.73 <math>\mu\text{m}</math></b>	Precalibrated <b>No</b>
Type:	Frame	Skew:	0
Fx:	4666.42	Cx:	2005.25
Fy:	4666.42	Cy:	1486.48
K1:	0.223613	P1:	0.00194777
K2:	0.373779	P2:	-0.00200162
K3:	1.24196	P3:	0
K4:	0	P4:	0

579  
 580  
 581  
 582  
 583  
 584  
 585

**3. Ground Control Points**



2 m

586  
587 **Fig. 3** GCP locations

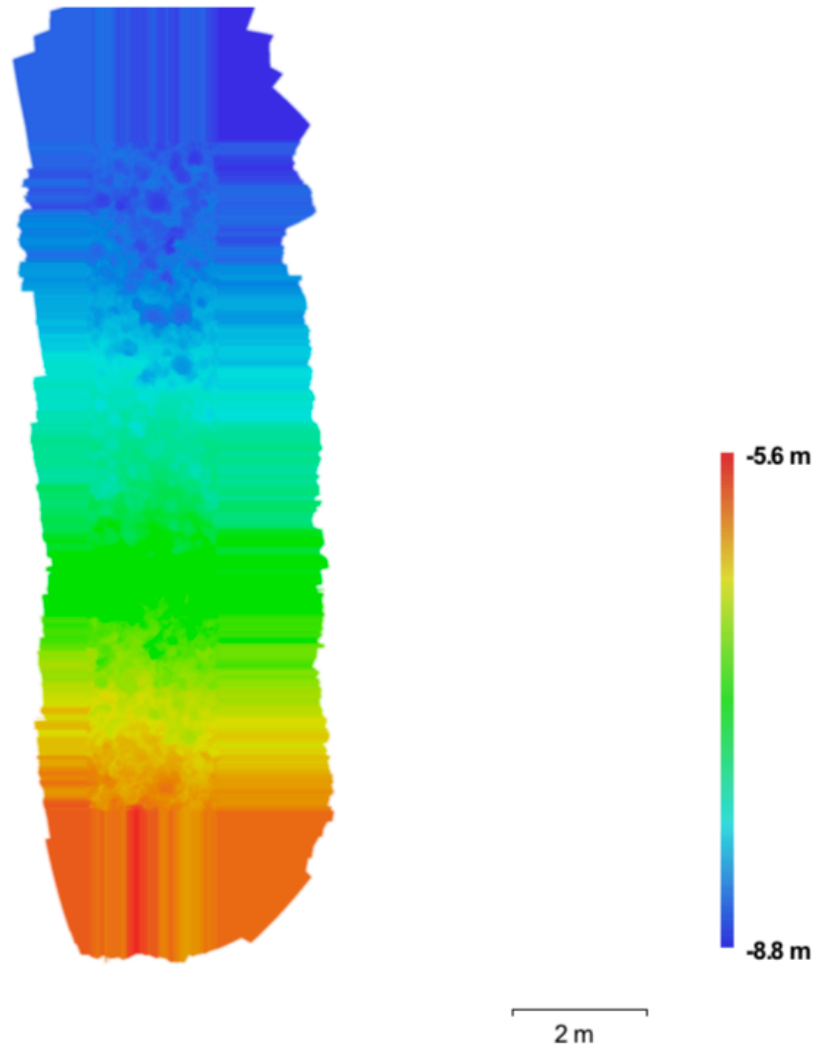
588  
589 **Tab. 2** Control points

Label	XY error(m)	Z error (m)	Error (m)	Projections	Error (pix)
point1	0.206298	-0.0677987	0.217153	13	1.992
point2	0.0963633	0.0426041	0.105361	16	1.153
point3	0.039409	3.96756e-05	0.039409	17	0.051
point4	0.205045	0.0251539	0.206582	9	0.044
<b>Total</b>	<b>0.154468</b>	<b>0.0419657</b>	<b>0.160067</b>		<b>1.151</b>

590  
591

592  
593

#### 4. Digital Elevation Model



594  
595  
596

**Fig. 4** Reconstructed digital elevation model.

Resolution: 1.06 mm/pix  
Point density: 889956 points per sq m

597  
598

599  
600

## 5. Processing parameters

### General

Cameras	157
Aligned cameras	157
Markers	4
Coordinate system	Local Coordinates

### Point Cloud

Points	139,838 of 221,231
RMS reprojection error	0.382302 (1.88392 pix)
Max reprojection error	6.30304 (30.1948 pix)
Mean key point size	5.32459 pix
Effective overlap	2.94411

### Alignment parameters

Accuracy	High
Pair preselection	Disabled
Key point limit	40,000
Tie point limit	4,000
Constrain features by mask	No
Matching time	17 minutes 46 seconds
Alignment time	3 minutes 10 seconds

### Optimization parameters

Parameters	f, cx, cy, k1-k3, p1, p2
Optimization time	5 seconds

### Dense Point Cloud

Points	72,229,238
--------	------------

### Reconstruction parameters

Quality	High
Depth filtering	Aggressive
Processing time	8 minutes 29 seconds

### Model

Faces	4,815,282
Vertices	2,417,898

### Reconstruction parameters

Surface type	Arbitrary
Source data	Dense
Interpolation	Enabled
Quality	High
Depth filtering	Aggressive
Face count	4,815,282
Processing time	4 hours 29 minutes

### DEM

Size	1,886 x 9,433
Coordinate system	Local Coordinates

### Reconstruction parameters

Source data	Dense cloud
Interpolation	Enabled

### Orthomosaic

Size	3,773 x 18,867
Coordinate system	Local Coordinates
Channels	3, unit8
Blending mode	Mosaic

### Reconstruction parameters

Surface	Mesh
Enable color correction	No

601